American Journal of Computational Mathematics, 2012, 2, 249-257
http://dx.doi.org/10.4236/ajcm.2012.24034 Published Online December 2012 (http://www.SciRP.org/journal/ajcm)

Application for Superconvergence of Finite Element Approximations for the Elliptic Problem by Global and Local L^2-Projection Methods

Rabeea H. Jari, Lin Mu
Department of Applied Science, UALR, Little Rock, USA
Email: rhjari@ualr.edu, lxmu@ualr.edu

Received February 12, 2012; revised May 21, 2012; accepted July 12, 2012

ABSTRACT

Numerical experiments are given to verify the theoretical results for superconvergence of the elliptic problem by global and local L^2-Projection methods.

Keywords: Finite Element Methods; Superconvergence; L^2-Projection; Elliptic Problem

1. Introduction

The elliptic problem seeks u in a certain functional space such that

$$-\Delta u = f \text{ in } \Omega \tag{1}$$

$$u = g \text{ in } \partial\Omega \tag{2}$$

where Δ denote the Laplacian operator.

Let T_h be a finite element partition of the domain Ω with characteristic mesh size h. Let $V_h \subset H_g^1(\Omega)$ be any finite element space for u associated with the partition T_h.

The L^2-Projection technique was introduced by Wang [1-3]. It projects the approximate solution to another finite element dimensional space associated with a coarse mesh.

Now, we start with defining a coarse mesh T_τ where $\tau \gg h$ satisfying:

$$\tau = h^\alpha \tag{3}$$

with $\alpha \in (0,1)$. Define finite element space $V_\tau \subset H^{s-2}(\Omega)$. Let Q_τ to be the L^2-Projector onto the finite element space V_τ [1,4,5]. The Projector Q_τ can be considered as a linear operator (projection) from $L^2(\Omega)$ onto the finite element space V_τ [6,7].

2. Superconvergence by Global L^2-Projection

The following theorems can be found in [1].

Theorem 2.1: Assume that $1 \le s \le k+1$ and the finite element space $V_\tau \subset H^{s-2}(\Omega)$. If the exact solution $u \in H^{k+1}(\Omega) \cap H^{r+1}(\Omega) \cap H_g^1(\Omega)$, then there exists a constant C such that

$$\|u - Q_\tau u_h\| + h^\alpha \|\nabla_\tau (u - Q_\tau u_h)\| \le Ch^{\alpha(r+1)}\|u\| + Ch^\sigma \|\nabla(u - u_h)\|,$$

where $\sigma = s - 1 + \alpha \min(0, 2-s)$ and u_h is the finite element approximation of (1) and (2).

Theorem 2.2: Suppose that $1 \le s \le k+1$. Let the surface fitting spaces $V_\tau \subset H^{s-2}(\Omega)$ and u_h be the finite element approximation of (1) and (2). Then, the post-processing of u_h is estimated by

$$\alpha = \frac{k+s-1}{r+1-\min(0,2-s)}.$$

3. Numerical Experiments for Global L^2-Projection

In this section, we present several numerical experiments to verify the theoretical analysis in [1]. The triangulation T_h is constructed by: 1) dividing the domain into an $n^3 \times n^3$ rectangular mesh; 2) connecting the diagonal line with the positive slope. Denote $h = \frac{1}{n^3}$ as the mesh size.

The finite element space is defined by

$$V_h = \left\{ v \in H_g^1(\Omega); v|_K \in P_1(K); \forall\, K \in T_h, v = g \text{ on } \partial\Omega \right\}.$$

We define V_τ as follows:

$$V_\tau = \left\{ v \in L^2(\Omega) : v|_K \in P_2(K); \forall\, K \in T_\tau \right\}.$$

Example 3.1: Let the domain $\Omega = [0,1] \times [0,1]$ and the exact solution is assumed as

$$u = x(1-x)y(1-y).$$

Table 1 shows that after the post-processing method, all the errors are reduced. The exact solution in L^2-norm of $\|u - Q_\tau u_h\|$ has the similar convergence rate as $\|u - u_h\|$. There is no improvement for the u in L^2-norm. However, the error in H^1-norm have higher convergence rate, which is shown as $O(h^{1.3})$ for $\|\nabla_\tau (u - Q_\tau u_h)\|$. The order of convergence rate is $O(h^{0.3})$ better than $\|\nabla(u - u_h)\|$, see **Figures 1(a)** and **(b)**.

Figures 2(a) and **(b)** give results for the finite element approximation of (1)-(2) before and after post-processing.

Example 3.2: Let the domain $\Omega = [0,1] \times [0,1]$ and the exact solution is assumed as

$$u = \sin(\pi x)\cos(\pi y).$$

Table 1. Errors on uniform triangular meshes T_h and T_τ.

h	$\lvert u-u_h \rvert_1$	$\|u-u_h\|$	$\lvert u-Qu_h \rvert_1$	$\|u-Qu_h\|$
2^{-3}	0.6632e−2	0.1287e−3	0.1427e−2	0.1227e−3
3^{-3}	0.2799e−2	0.2295e−4	0.4332e−3	0.2185e−4
4^{-3}	0.1433e−2	0.6017e−5	0.1763e−3	0.5730e−5
5^{-3}	0.8294e−3	0.2015e−5	0.8504e−4	0.1919e−5
6^{-3}	0.5223e−3	0.7992e−6	0.4596e−4	0.7610e−6
$O(h)$	0.9998	1.9993	1.3504	1.9996

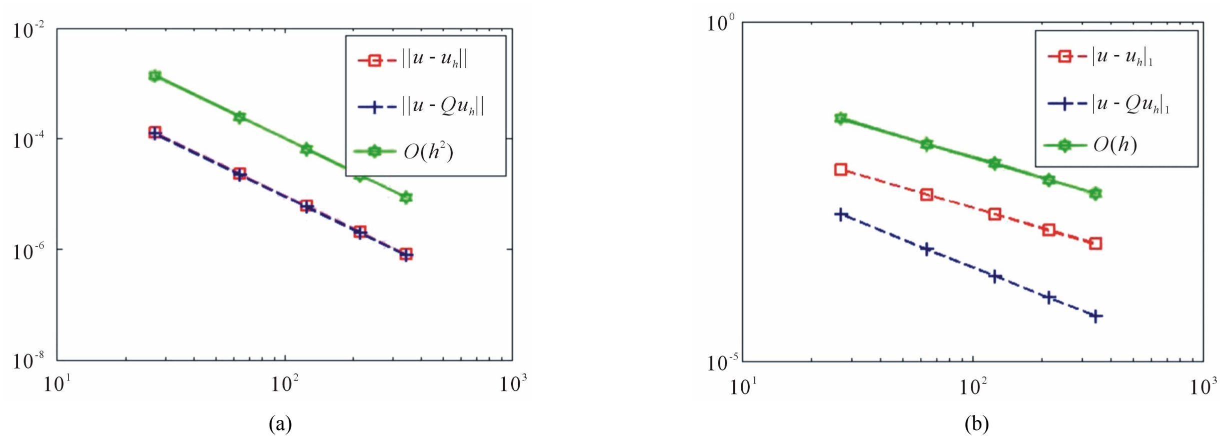

Figure 1. (a) Convergence rate of L^2-norm error; (b) Convergence rate of H^1-norm error.

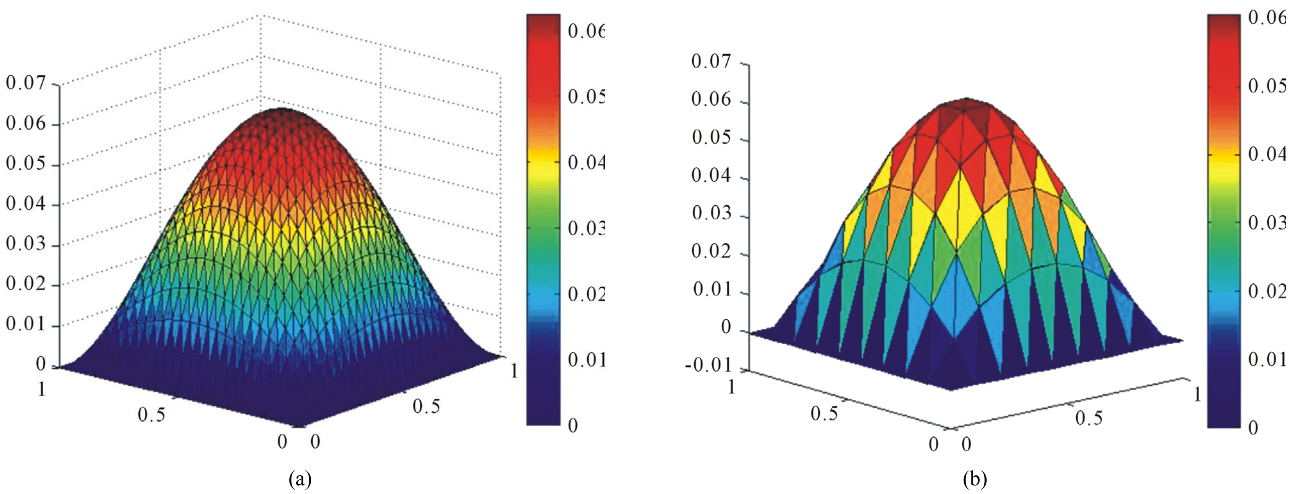

Figure 2. (a) Surface plot of approximation solution u_h; (b) Surface plot of approximation solution $Q_\tau u_h$.

From the results shown in **Table 2**, it is clear that the exact solution u in H^1-norm has the superconvergence, but there is no improvement in the L^2-norm, see **Figures 3(a)** and **(b)**. The finite element solution given in **Figures 4(a)** and **(b)**. This agrees well with the theory.

Example 3.3: Let the domain $\Omega=[0,1]\times[0,1]$ and the exact solution is assumed as

$$u=\frac{\cos(\pi(x+y))}{2}.$$

Table 3 gives the errors profile for Example 3. Notice that, the gradient estimate is of order $O(h^{1.3})$, that is much better than the optimal order $O(h)$. Although, there is no improvement in the L^2-norm, see **Figure 5**.

Figure 6 shows that the approximation solutions u_h and $Q_\tau u_h$.

Also, our numerical results and theoretical conclusions in Theorems (2.1) and (2.2) show highly consistent.

Table 2. Errors on uniform triangular meshes T_h and T_τ.

h	$\lvert u-u_h\rvert_1$	$\lVert u-u_h\rVert$	$\lvert u-Qu_h\rvert_1$	$\lVert u-Qu_h\rVert$
2^{-3}	0.9629e−1	0.1598e−2	0.2242e−1	0.1498e−2
3^{-3}	0.4063e−1	0.2850e−3	0.6872e−2	0.2669e−3
4^{-3}	0.2080e−1	0.7475e−4	0.2810e−2	0.6998e−4
5^{-3}	0.1204e−1	0.2503e−4	0.1359e−2	0.2343e−4
6^{-3}	0.7582e−2	0.9929e−5	0.7363e−3	0.9294e−5
$O(h)$	0.9998	1.9991	1.3427	1.9995

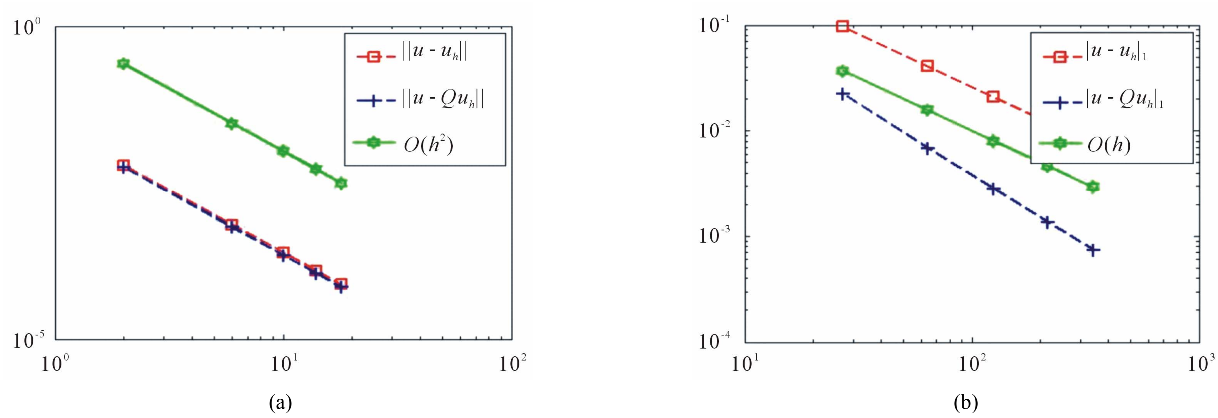

Figure 3. (a) Convergence rate of error L^2-norm error; (b) Convergence rate of H^1-norm error.

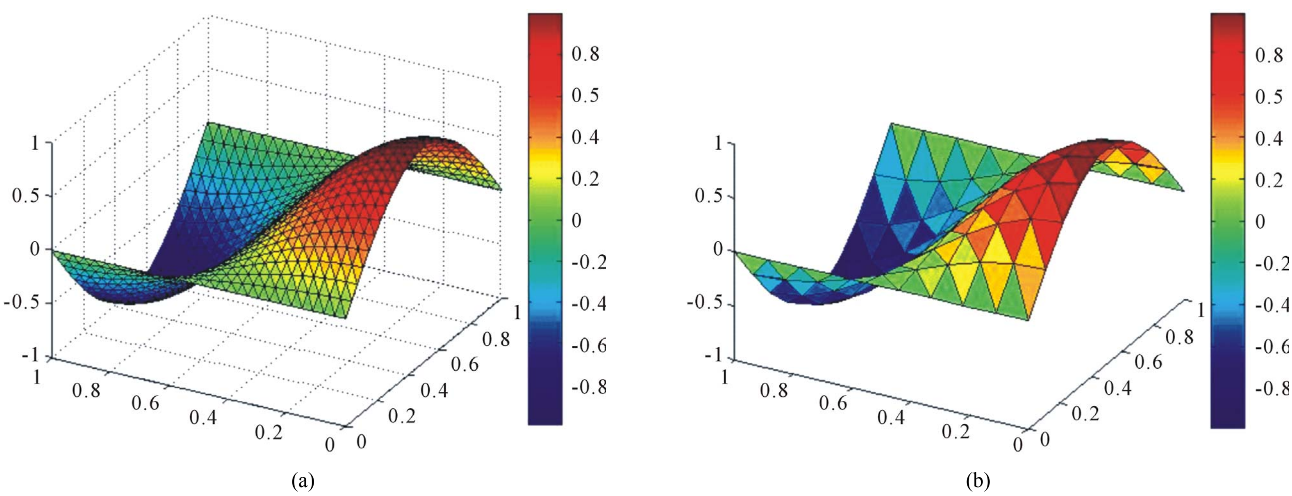

Figure 4. (a) Surface plot of solution u_h; (b) Surface plot of approximation solution $Q_\tau u_h$.

Table 3. Errors on uniform triangular meshes T_h and T_τ.

h	$\lvert u-u_h\rvert_1$	$\lVert u-u_h\rVert$	$\lvert u-Qu_h\rvert_1$	$\lVert u-Qu_h\rVert$
2^{-3}	0.9135e−1	0.1770e−2	0.2150e−1	0.1689e−2
3^{-3}	0.3855e−1	0.3157e−3	0.6579e−2	0.3010e−3
4^{-3}	0.1973e−1	0.8278e−4	0.2692e−2	0.7893e−4
5^{-3}	0.1142e−1	0.2772e−4	0.1303e−2	0.2643e−4
6^{-3}	0.7193e−2	0.1099e−4	0.7062e−3	0.1048e−4
$O(h)$	0.9999	1.9993	1.3424	1.9994

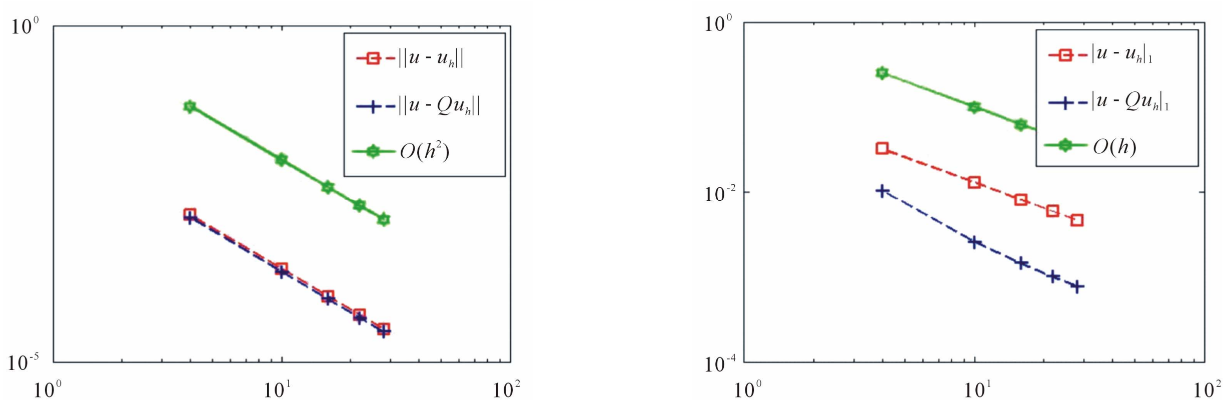

(a) (b)

Figure 5. (a) Convergence rate of L^2-norm error; (b) Convergence rate of H^1-norm error.

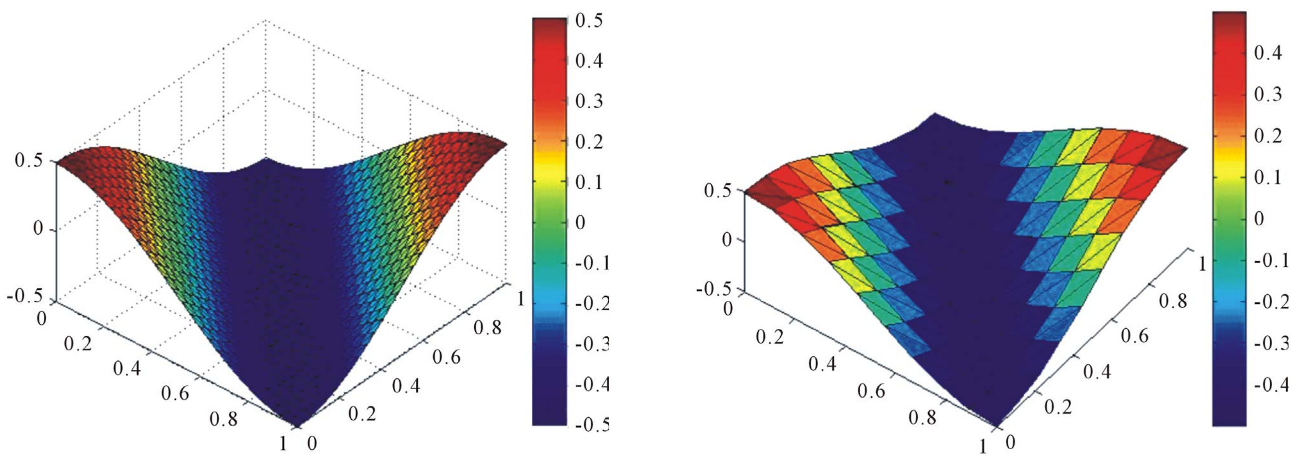

(a) (b)

Figure 6. (a) Surface plot of approximation solution u_h; (b) Surface plot of approximation solution $Q_\tau u_h$.

4. Superconvergence by Local L^2-Projection

Notice that, the exact solution u may be not smooth globally on Ω in practical computation, although the solution might be smooth enough locally for a good super convergence.

To this end, let Ω_0 be a subdomain of Ω where the exact solution u is sufficiently smooth. Let Ω_1 be another subdomain of Ω such that $\Omega_0 \subset \Omega_1$. Define finite element space $V_\tau \subset H^{s-2}(\Omega_1)$ The L^2-projection Q_τ from $L^2(\Omega)$ onto the finite element space V_τ is said to be local L^2-projection.

The following theorem can be found in [1].

Theorem 4.1: Assume that $1 \le s \le k+1$ and the finite element space $V_\tau \subset H^{s-2}(\Omega_0)$. If the exact solution $u \in H^{k+1}(\Omega) \cap H^{r+1}(\Omega_0) \cap H_g^1(\Omega)$, then there exists a constant C such that

$$\left\|u-Q_\tau u_h\right\|_{\Omega_0}+h^\alpha\left\|\nabla_\tau\left(u-Q_\tau u_h\right)\right\|_{\Omega_0} \le Ch^{\alpha(r+1)}\left\|u\right\|_{\Omega_0}+Ch^\alpha\left\|\nabla\left(u-u_h\right)\right\|_{\Omega_0},$$

where u_h is the finite element approximation of (1)-(2).

Theorem 4.2: Suppose that $1\le s\le k+1$. Let the surface fitting spaces $V_\tau\subset H^{s-2}\left(\Omega_0\right)$ and u_h be the finite element approximation of (1)-(2). Then, the post-processing of u_h is estimated by

$$\alpha=\frac{k+s-1}{r+1-\min\left(0,2-s\right)}.$$

5. Numerical Experiments for Local L^2-Projection

In this section, we present several numerical experiments to verify the theoretical analysis in [1]. The triangulation T_h is constructed by: 1) dividing the domain into an $n^3\times n^3$ rectangular mesh; 2) connecting the diagonal line with the positive slope. Denote $h=\frac{1}{n^3}$ as the mesh size.

The finite element space is defined by

$$V_h=\left\{v\in H_g^1\left(\Omega\right);v|_K\in P_1\left(K\right);\forall K\in T_h,v=g\text{ on }\partial\Omega\right\}.$$

We define V_τ as follows:

$$V_\tau=\left\{v\in L^2\left(\Omega\right):v|_K\in P_2\left(K\right);\forall K\in T_\tau\right\}.$$

Example 5.1: Let the domain $\Omega=\left[0,1\right]\times\left[0,1\right]$ and $\Omega_0=\left[0,0.5\right]\times\left[0,0.5\right]$. The exact solution is assumed as

$$u=\frac{1}{2-x-y}.$$

It is clear that the exact solution u is singular and f blows down at the boundary of $\Omega=\left[0,1\right]\times\left[0,1\right]$, see **Figure 7**, however, u_h and $Q_\tau u_h$ are sufficiently smooth on $\Omega=\left[0,1\right]\times\left[0,1\right]$, see **Figure 8**.

Table 4 shows that after the post-processing method, all the errors are reduced. The exact solution in L^2-norm of $\left\|u-Q_\tau u_h\right\|$ has the similar convergence rate as $\left\|u-u_h\right\|$ which is shown as $O\left(h^2\right)$. There is no improvement for the u in L^2-norm. However, the error in H^1-norm have higher convergence rate, which is shown as $O\left(h^{1.3}\right)$ for $\left\|\nabla_\tau\left(u-Q_\tau u_h\right)\right\|$. The order of convergence rate is $O\left(h^{0.3}\right)$ better than $\left\|\nabla_h\left(u-u_h\right)\right\|$, see **Figure 9.**

Example 5.2: Let the domain $\Omega=\left[0,1\right]\times\left[0,1\right]$ and $\Omega_0=\left[0.5,1\right]\times\left[0.5,1\right]$. The exact solution is assumed as

$$u=\sqrt{x^2+y^2}$$

Obviously, the exact solution has singularity on the origin at the domain $\Omega=\left[0,1\right]\times\left[0,1\right]$, see **Figure 10(a)**. On the same domain the function f blows down at the boundary, see **Figure 10(b)**. The approximation solutions u and $Q_\tau u_h$ have been plot in the proper subdomain $\Omega_0=\left[0.5,1\right]\times\left[0.5,1\right]$, see **Figure 11**.

From the results shown in **Table 5**, it is clear that the exact u in H^1-norm has the superconvergence, but there is no improvement in the L^2-norm, see **Figure 12**. This agrees well with the theory.

Example 6: Let the domain $\Omega=\left[0,1\right]\times\left[0,1\right]$ and $\Omega_0=\left[0.5,1\right]\times\left[0.5,1\right]$. The exact solution is assumed as

$$u=\frac{y}{\sqrt{x^2+y^2}}.$$

From **Figures 13(a)** and **(b)**, respectively observe that the exact solution has strongly singularity on the origin of the domain $\Omega=\left[0,1\right]\times\left[0,1\right]$ and the function f blows up at the boundary, **Figure 14** show how the approximation solution u_h and $Q_\tau u_h$ look like at the proper subdomain $\Omega_0=\left[0.5,1\right]\times\left[0.5,1\right]$.

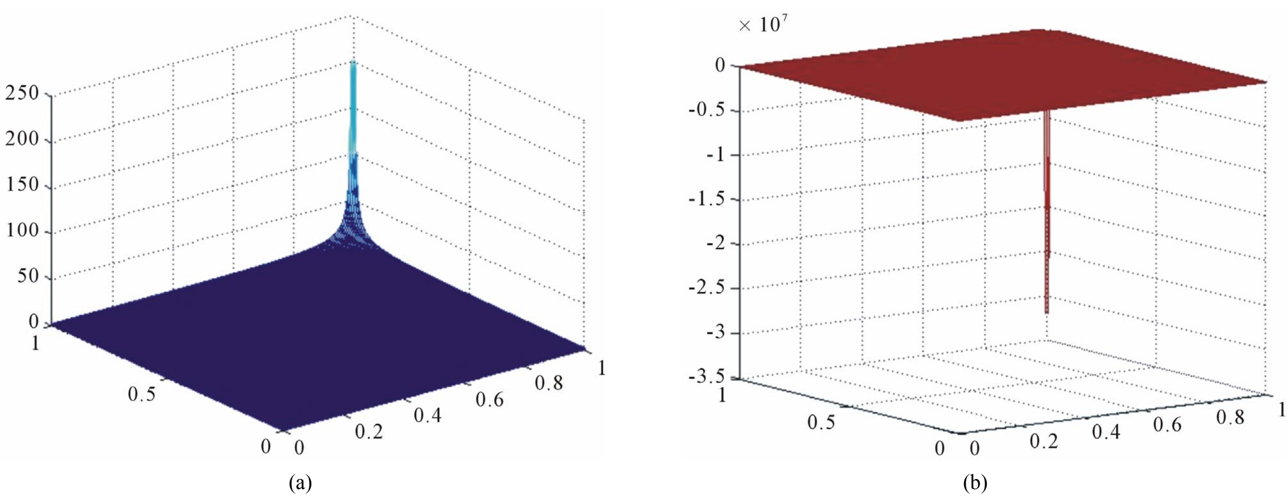

Figure 7. (a) The exact solution *u* blows up; (b) *f* blows down at the boundary.

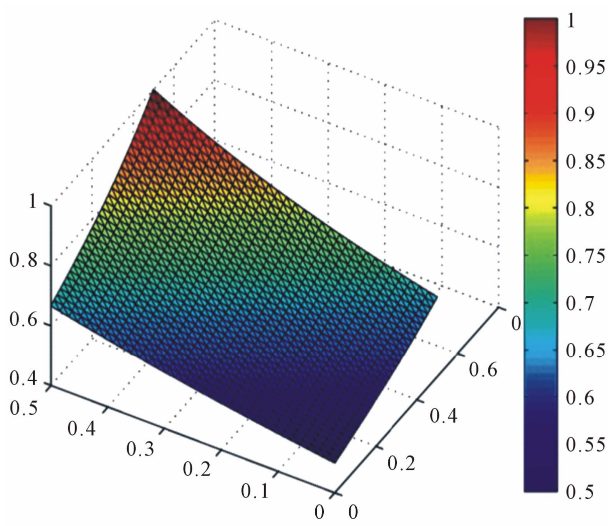

(a)

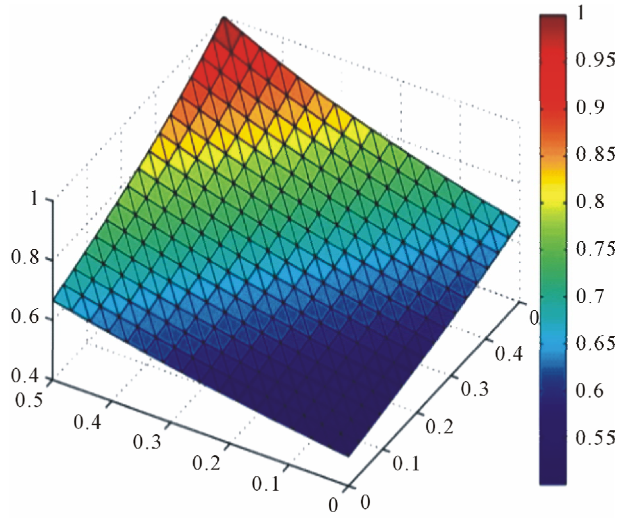

(b)

Figure 8. (a) Surface plot of approximation solution u_h; (b) Surface plot of approximation solution $Q_\tau u_h$.

Table 4. Errors on uniform triangular meshes T_h and T_τ.

h	$\lvert u-u_h\rvert_1$	$\lVert u-u_h\rVert$	$\lvert u-Qu_h\rvert_1$	$\lVert u-Qu_h\rVert$
2^{-3}	0.3221e−1	0.1497e−2	0.1026e−1	0.1363e−2
3^{-3}	0.1291e−1	0.2384e−3	0.2566e−2	0.2169e−3
4^{-3}	0.8072e−2	0.9306e−4	0.1429e−2	0.8466e−4
5^{-3}	0.5871e−2	0.4921e−4	0.9977e−3	0.4476e−4
6^{-3}	0.4613e−2	0.3037e−4	0.7691e−3	0.2763e−4
$O(h)$	0.9998	2.0030	1.3360	2.0035

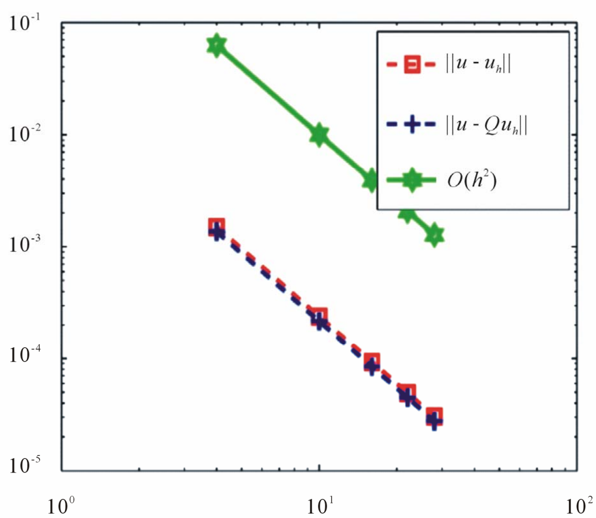

(a)

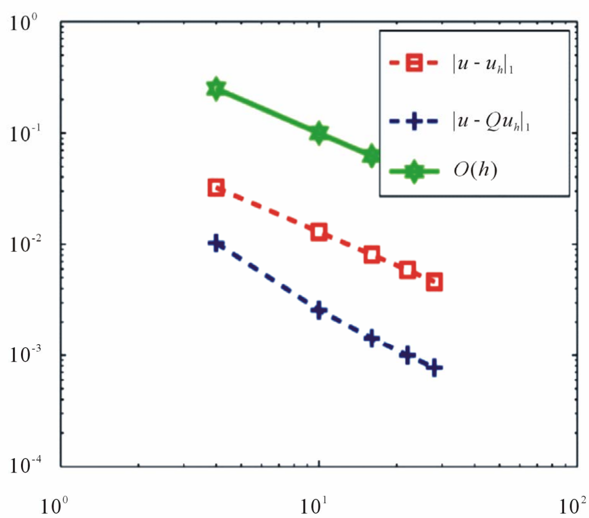

(b)

Figure 9. (a) Convergence rate of L^2-norm error; (b) Convergence rate of H^1-norm error.

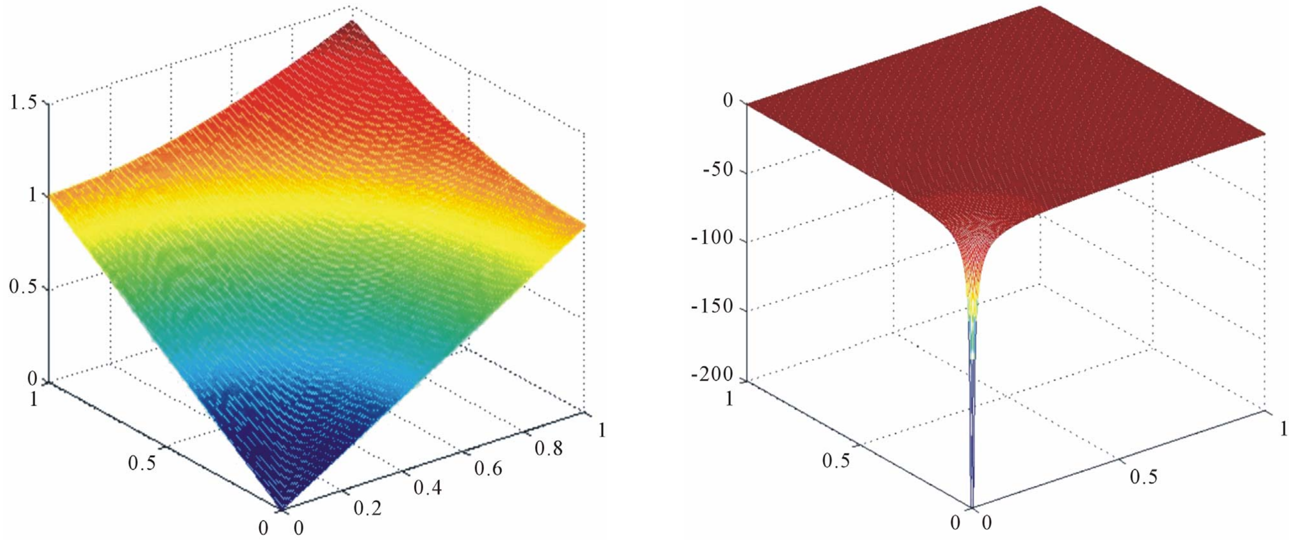

(a) (b)

Figure 10. (a) Surface plot of exact solution u; (b) f blows down at the boundary.

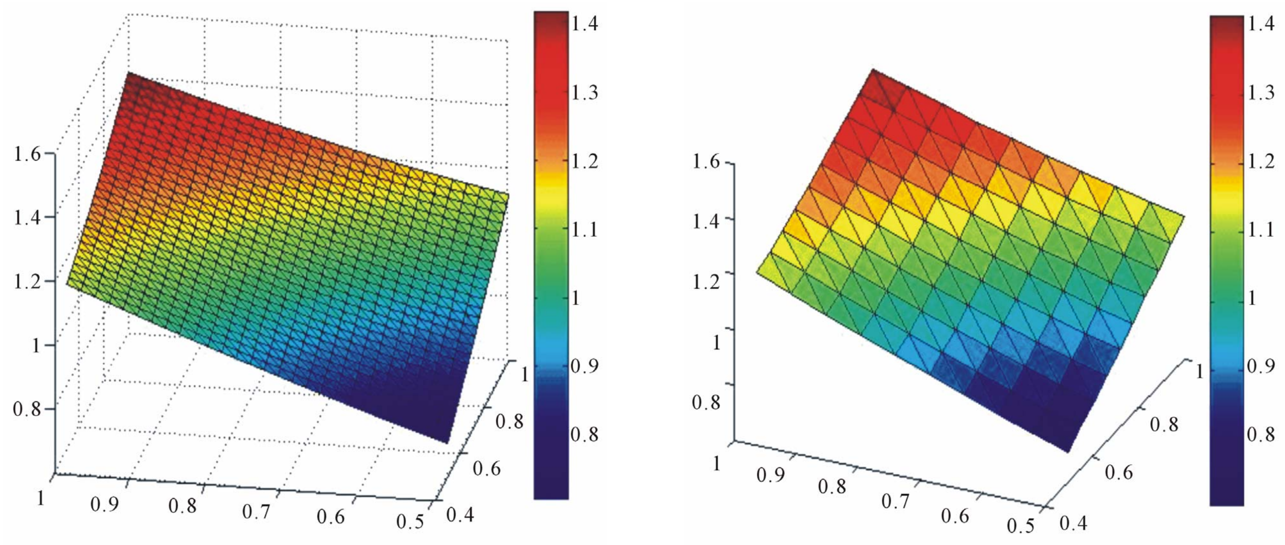

(a) (b)

Figure 11. (a) Surface plot of approximation solution u_h; (b) Surface plot of approximation solution $Q_\tau u_h$.

Table 5. Errors on uniform triangular meshes T_h and T_τ.

h	$\lvert u-u_h \rvert_1$	$\lVert u-u_h \rVert$	$\lvert u-Qu_h \rvert_1$	$\lVert u-Qu_h \rVert$
2^{-3}	0.1352e−1	0.1400e−2	0.6141e−2	0.1287e−2
3^{-3}	0.6835e−2	0.3596e−3	0.2110e−2	0.3314e−3
4^{-3}	0.4566e−2	0.1607e−3	0.1215e−2	0.1481e−3
5^{-3}	0.3427e−2	0.9058e−4	0.8529e−3	0.8352e−4
6^{-3}	0.2743e−2	0.5802e−4	0.6590e−3	0.5350e−4
$O(h)$	0.9923	1.9806	1.3581	1.9792

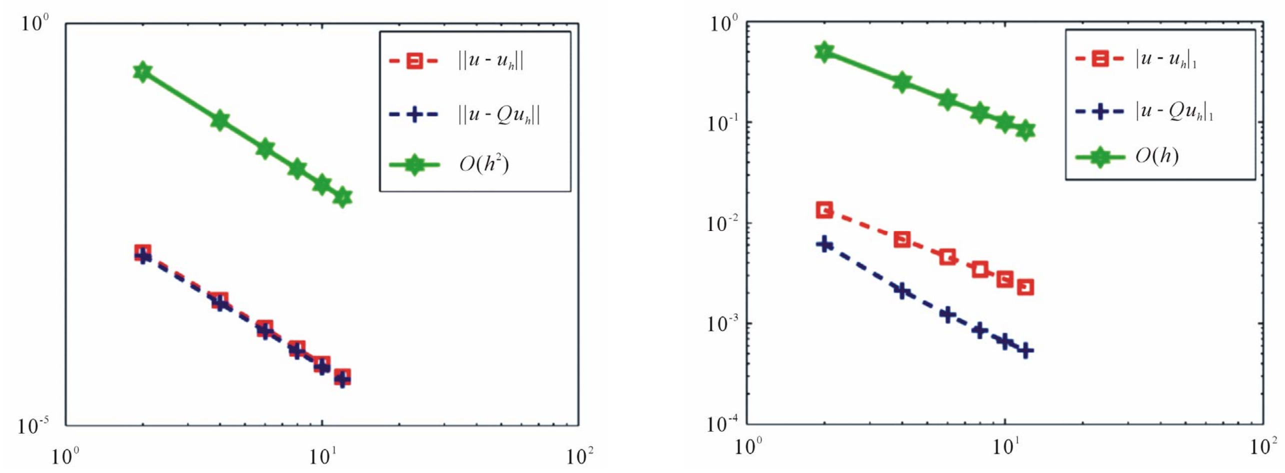

(a) (b)

Figure 12. (a) Convergence rate of L^2-norm error; (b) Convergence rate of H^1-norm error.

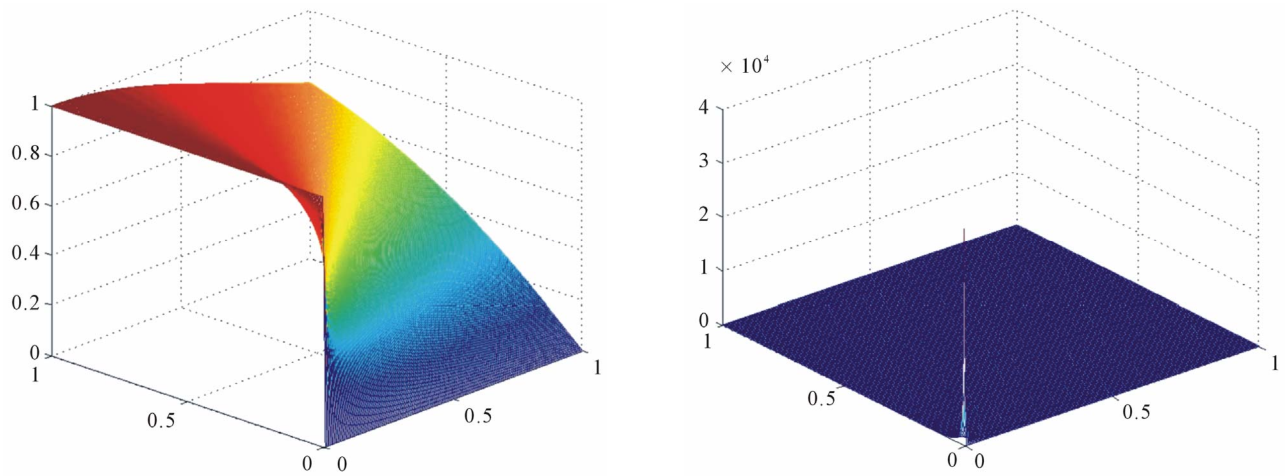

(a) (b)

Figure 13. (a) Surface plot of exact solution u; (b) f blows up at the boundary.

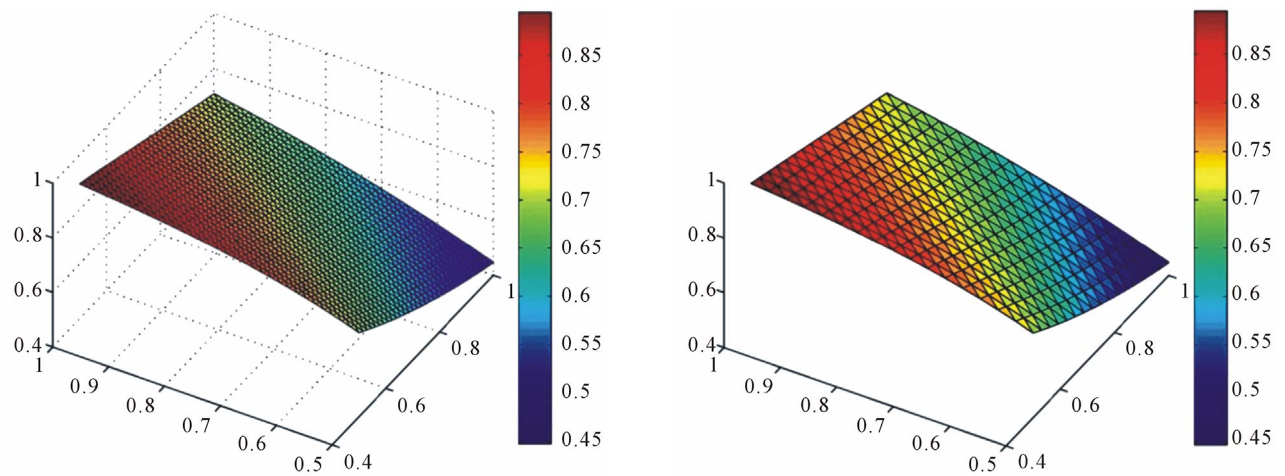

(a) (b)

Figure 14. (a) Surface plot of approximation solution u_h; (b) Surface plot of approximation solution $Q_\tau u_h$.

Table 6. Errors on uniform triangular meshes T_h and T_τ.

h	$\lvert u-u_h\rvert_1$	$\lVert u-u_h\rVert$	$\lvert u-Qu_h\rvert_1$	$\lVert u-Qu_h\rVert$
2^{-3}	0.1186e−1	0.4006e−3	0.4708e−2	0.2779e−3
3^{-3}	0.5979e−2	0.1009e−3	0.1621e−2	0.6959e−4
4^{-3}	0.3992e−2	0.4490e−4	0.9518e−3	0.3094e−4
5^{-3}	0.2996e−2	0.2527e−4	0.6760e−3	0.1740e−4
6^{-3}	0.2397e−2	0.1617e−4	0.5261e−3	0.1113e−4
$O(h)$	0.9943	1.9949	1.3304	1.9989

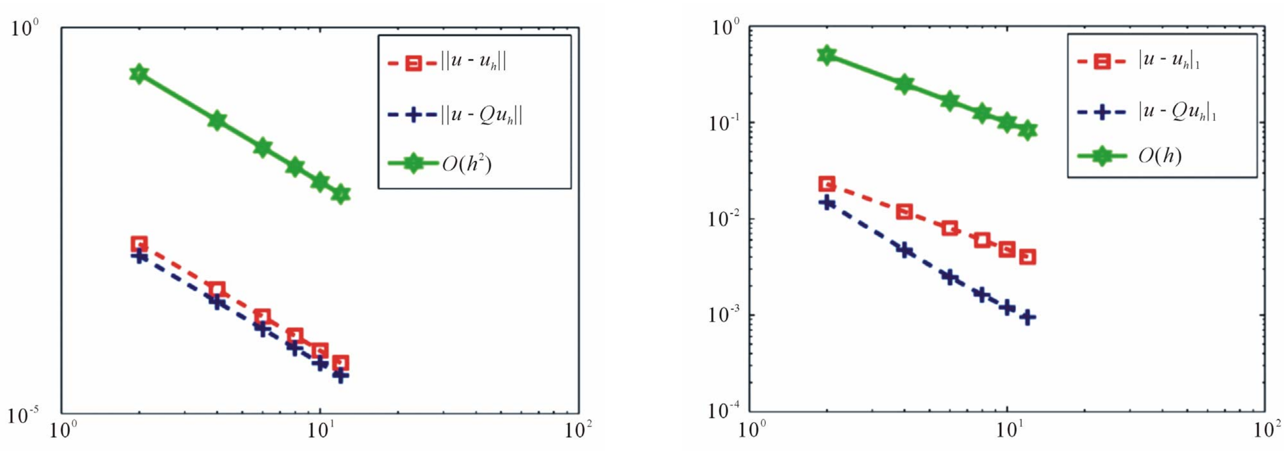

(a) (b)

Figure 15. (a) Convergence rate of L^2-norm error; (b) Convergence rate of H^1-norm error.

Table 6 gives the errors profile for Example 6. Notice that, the gradient estimate is of order $O(h^{1.3})$ that is much better than the optimal order $O(h)$. Although, there is no improvement in the L^2-norm, see **Figure 15**. Also, the numerical results and theoretical conclusions show highly consistent.

REFERENCES

[1] J. Wang, "A Superconvergence Analysis for Finite Element Solutions by the Least-Squares Surface Fitting on Irregular Meshes for Smooth Problems," *Journal of Mathematical Study*, Vol. 33, No. 3, 2000, pp. 229-243.

[2] R. E. Ewing, R. Lazarov and J. Wang, "Superconvergence of the Velocity along the Gauss Lines in Mixed Finite Element Methods," *SIAM Journal on Numerical Analysis*, Vol. 28, No. 4, 1991, pp. 1015-1029. doi:10.1137/0728054

[3] M. Zlamal, "Superconvergence and Reduced Integration in the Finite Element Method," *Mathematics Computation*, Vol. 32, No. 143, 1977, pp. 663-685. doi:10.2307/2006479

[4] L. B. Wahlbin, "Superconvergence in Galerkin Finite Element Methods," Lecture Notes in Mathematics, Springer, Berlin, 1995.

[5] A. H. Schatz, I. H. Sloan and L. B. Wahlbin, "Superconvergence in Finite Element Methods and Meshes that Are Symmetric with Respect to a Point," *SIAM Journal on Numerical Analysis*, Vol. 33, No. 2, 1996, pp. 505-521. doi:10.1137/0733027

[6] M. Krizaek and P. Neittaanmaki, "Superconvergence Phenomenon in the Finite Element Method Arising from Avaraging Gradients," *Numerische Mathematik*, Vol. 45, No. 1, 1984, pp. 105-116.

[7] J. Douglas and T. Dupont, "Superconvergence for Galerkin Methods for the Two-Point Boundary Problem via Local Projections," *Numerical Mathematics*, Vol. 21, No. 3, 1973, pp. 270-278. doi:10.1007/BF01436631